A MACROSCOPIC TRANSIENT MODEL FOR SIMULATING ALVEOLAR GAS DIFFUSION

José L. Lage - JLL@SEAS.SMU.EDU
Mechanical Engineering Department
Southern Methodist University
Dallas, Texas, 75275-0337
Vladimir V. Kulish - mvvkulish@ntu.edu.sg
School of Mechanical & Production Engineering
Nanyang Technological University
50 Nanyang Ave., Singapore 639798
Connie C. W. Hsia - CONNIE.HSIA@email.swmed.edu
Department of Internal Medicine
University of Texas - Southwestern Medical Center
Dallas, Texas, 75235-9034
Robert L. Johnson, Jr. - ROBERT.JOHNSON@email.swmed.edu
Department of Internal Medicine
University of Texas - Southwestern Medical Center
Dallas, Texas, 75235-9034

Abstract. *A novel mathematical model derived from fundamental engineering principles for simulating the spatial and temporal gas diffusion process within the alveolar region of the lung was presented recently by Koulich et al. (1999). The model depends on a physical property of the alveolar region termed effective diffusivity, function of the diffusivity, solubility, and interface geometry of each alveolar constituent. Unfortunately, the direct determination of the effective diffusivity of the alveolar region is impractical because of the difficulty in describing the internal geometry of each alveolar constituent. However, the transient solution of the macroscopic model can be used in conjunction with the lung diffusing capacity (measured in laboratory via the single-breath technique) to determine the effective diffusivity of the alveolar region. With the effective diffusivity known, the three-dimensional effects of red blood cell distribution on the lung diffusing capacity can be predicted via numerical simulations. The results, obtained for normal (random), uniform, center-cluster, corner-cluster, and several chain-like distributions, unveil a strong relationship between the type of cell distribution and the lung diffusing capacity.*

Keywords: mass diffusion, lung diffusing capacity, alveolus, macroscopic model, transient simulation

1. INTRODUCTION

The search for a universal correlation between the lung diffusing capacity and the physical properties of each individual lung alveolar constituent (e.g., membranes, tissue,

plasma, red blood cells, etc.) has been a major research trust (Roughton and Foster, 1957; Weibel, 1970; Crapo and Crapo, 1983; Crapo et al., 1988; Fedrespiel, 1989; Weibel et al., 1993). Existing theories for estimating the lung diffusing capacity are limited by the difficulty in characterizing the incredibly complex internal geometry (morphology) of the alveolar region, including the distribution of red blood cells within the capillary bed (Hsia et al., 1995).

The lung diffusing capacity, as defined, is a lumped parameter that can be estimated from relatively simple measurements (Johnson et al., 1960; Newth et al., 1977; American Thoracic Society, 1987) and used to indicate abnormalities in the respiratory diffusion process. However, it is difficult to infer from variations in the lung diffusing capacity the precise cause of the abnormality because the sensitivity of the lung diffusing capacity (a global parameter) to local changes in the functionality of the lung is not well known. There is a need for linking the local diffusion process occurring within the alveolar region to the measurable variations in the global lung diffusing capacity parameter.

These observations provide grounds for seeking the development of suitable models that simulate locally the gas diffusion process inside the alveolar region of the lung. Unfortunately, using the classical gas diffusion equation at the alveolus-erythrocyte level (referred here as the microscopic level) within a lung is impractical because: (1) the dimensional scale of the domain ranges from decimeters to microns, requiring a tremendous numerical resolution, and, more importantly, (2) the complex internal alveolar structure (topology) is extremely difficult to access and to map.

A novel macroscopic model for simulating the gas diffusion within the alveolar region of the lung, overcoming the scale and structure difficulties, was presented recently by Koulich et al. (1999). A by-product of this model is the introduction of a macroscopic transport property of the alveolar region, called effective diffusivity. As defined, this property depends on the internal structure of the alveolar region, bringing back the very same structure-related problem the model originally tried to overcome.

However, it is possible to determine the equivalent effective diffusivity of the alveolar region by simulating numerically the single-breath CO-diffusion procedure done in the laboratory and comparing the lung diffusing capacity obtained from the numerical results to the lung diffusing capacity obtained experimentally. Once determined, the effective diffusivity can be used with the three-dimensional, transient macroscopic diffusion model to investigate the effects of red cell distribution on the lung diffusing capacity.

2.   MATHEMATICAL MODELING

The macroscopic diffusion equation derived by Koulich et al. (1999) is

$$\frac{\partial \langle P \rangle}{\partial t} = D_{eff} \nabla^2 \langle P \rangle \qquad (1)$$

where $\langle P \rangle$ is the macroscopic effective partial-pressure of the gas being considered during the diffusion process inside the alveolar region, t is the time, and D_{eff} is the effective diffusivity of the alveolar region. Recall that the macroscopic effective partial-pressure $\langle P \rangle$ is defined as the volume-averaged of the diffusing gas partial-pressure within an elementary volume representative of the alveolar region. This elementary representative volume contains all the constituents of the alveolar region, except the interior of the red blood cells. In fact, as explained by Koulich et al. (1999), the interface between the interior red cell and the red cell

membrane is considered as an interior boundary of the numerical domain where a boundary condition must be imposed.

Observe that once D_{eff} is known, Eq. (1) can be solved easily by applying suitable initial and boundary conditions. Therefore, there is no need to describe the internal structure of the alveolar region when using Eq. (1). The structure-information is now embedded into D_{eff}. The difficulty is then transferred from modeling the mass diffusion process per se to determining the effective diffusivity of the medium as a function of the structure and physical (molecular) properties of each constituent within the alveolar region. Unfortunately, the mathematical description of D_{eff} is very complex (Koulich et al., 1999), involving the precise mapping of all boundaries of each constituent within the alveolar region.

The lung diffusing capacity obtained in laboratory results from unsteady processes, such as the diffusion process during the single-breath technique (Comroe et al. 1962, p.122). This technique consists of having a subject inspiring a certain gas mixture with a low concentration of CO, and holding it in for a certain period of time (generally ten seconds). During this time, CO will diffuse from the alveolus region to the RBC's. The process is unsteady because the potential gradient driving the diffusion varies in time. The ratio between the volumetric amount of CO absorbed per unit of time and the difference between initial and final volume-averaged CO partial-pressure provides a measure of the lung diffusing capacity.

It is necessary, then, to model the diffusion process as occurring during the experimental measurement of D_L. Unfortunately, this means that the transient term of the macroscopic model Eq. (1) must be retained. The model equation becomes then dependent on D_{eff}, a quantity not known a priori.

Not everything is lost, however. By mimicking the experimental procedure, numerical simulations can be used to determine the correct value of the effective diffusivity that yields, from the numerical results, the same lung diffusing capacity value as the one found experimentally.

In the next two sections we present an overview of the lung diffusing capacity calculations behind the single-breath technique and a procedure to find the equivalent effective diffusivity of the alveolar region.

3. SINGLE-BREATH TECHNIQUE

The lung diffusing capacity of the alveolar region can be obtained from the single-breath technique results using the Krogh equation (Comroe et al., 1962, p.351)

$$\langle P \rangle_v (t) = \langle P \rangle_{v0} \; e^{-\left(\frac{D_L P_{ref}}{V_A} \right) t} \tag{2}$$

where $\langle P \rangle_{v0}$ is the initial value of the volume-averaged partial-pressure, the reference pressure P_{ref} is chosen as the total pressure of dry gases (equal to 9.51×10^4 Pa, or 713 mm Hg), and V_A is the alveolar volume equal to the inspired volume plus the residual lung volume (a representative, normal, value for V_A is 4,930 ml STPD). This equation can be derived from a lumped capacity approach to the diffusion process inside the alveolar region.

The characteristic time constant for the diffusion process, according to Eq. (2), is $V_A/(D_L P_{ref})$, typically equal to 24.4 s (using V_A = 4,930 ml, D_L = 17 ml$_{CO}$/mmHg min, and P_{ref} = 713 mmHg). This means that it takes approximately 25 seconds for the volume-averaged partial-pressure of CO (or concentration) in the lungs to be reduced to 37.3 percent of the

initial value. Notice that using the diffusion and solubility laws (Comroe et al., 1962, p. 350), it is possible to show that the lung diffusing capacity of oxygen is about 1.23 times the diffusing capacity of carbon monoxide. Therefore, the corresponding characteristic time for diffusion of oxygen is approximately equal to 20 seconds.

The lung diffusing capacity can be obtained easily from the partial-pressure results, by rearranging Eq. (2)

$$D_L = \frac{V_A}{P_{ref}\, t} ln\left[\frac{\langle P \rangle_v (0)}{\langle P \rangle_v (t)} \right] \tag{3}$$

During clinical single-breath tests, Eq. (3) is used for determining the lung diffusing capacity.

It is easy to determine a condition for the validity of the lumped capacity approach (and the validity of the Krogh equation) by considering the definition of the lung diffusing capacity as equivalent to the definition of mass transfer coefficient from Newton's Law of cooling. In this context, one has

$$\frac{c_{ref}\, RT}{M} \frac{\ell}{A} \frac{D_L}{D_{eff}} \sim P_{ref} \frac{\ell}{A} \frac{D_L}{D_{eff}} < 1 \tag{4}$$

4. ITERATIVE NUMERICAL SCHEME

The value of the effective diffusivity equivalent to a lung diffusing value obtained in the laboratory can be found by using an iterative numerical approach as explained next.

Equation (1) can be used to simulate the diffusion process during the single-breath test, for instance, but it is necessary to know a value for D_{eff}.

As a first guess, the D_{eff} value obtained from the steady-state analysis of Koulich et al. (1999) can be used with Eq. (1) to determine the time-evolution of the volume-averaged CO partial-pressure. Once the results are obtained, a lung diffusing capacity D_L can be found from Eq. (3). This value is not expected to match the lung diffusing capacity found experimentally, because the initial D_{eff} value (obtained from steady-state results) was just an approximation to the correct value. Therefore, a new guess for D_{eff} is used to simulate again the diffusion process. The new results yield a new value of D_L to be compare against the experimental value. A predictor-corrector iteration scheme can then be used to fine-tune the D_{eff} value used in Eq. (1) until the correct (measurable) D_L value is obtained from the numerical results.

5. TRANSIENT SIMULATIONS: NORMAL DISTRIBUTION

Transient numerical simulations of alveolar CO diffusion is performed by discretising Eq. (1) using finite differences, and solving the algebraic equations within a representative alveolar cubic domain. The initial condition is $\langle P \rangle (t) = \langle P \rangle_0 = 133.3$ Pa ($= 1$ Torr) everywhere within the cubic domain, except at the RBC locations where the partial-pressure of CO is always equal to zero, i.e., $\langle P \rangle_h = 0$. The domain boundary is set as impermeable to gas diffusion, therefore, $\partial \langle P \rangle / \partial n = 0$ at the boundary, where n is the coordinate along the direction normal to the boundary. The red cell density is $\rho = 0.034$, and the cells are distributed randomly (normal distribution) within the domain. Additional details of the

numerical procedure can be found in Koulich (1999).

The estimated effective diffusivity found numerically by Koulich et al. (1999) from the steady-state analysis, $D_{eff} = 9.4 \times 10^{-8}$ m^2/s, is used in Eq. (1) as a first guess to simulate the transient process within the alveolar region. After several iterations, it is found that $D_{eff} = 2.68 \times 10^{-7}$ m^2/s yields results from which D_L, obtained from Eq. (3), matches the value $D_L = 17$ ml$_{CO}$/(min mmHg) to within one percent.

The corresponding time-evolution of $\langle P \rangle$, obtained with $D_{eff} = 2.68 \times 10^{-7}$ m^2/s, is shown on Fig. 1 in terms of γ, where

$$\gamma = ln\left[\langle P \rangle_{v_0} / \langle P \rangle_v (t)\right] \tag{5}$$

The results shown in Fig. 1 are very similar to the results obtained experimentally using the single-breath technique for measuring the lung diffusing capacity. Observe that the time decay of the volume-averaged CO partial-pressure seems to follow an exponential curve.

It is now possible to re-visit the criterion for the validity of Eq. (3). Quantitatively, one has $P_{ref} \sim 10^5$ Pa, $\ell/A \sim 10^{-5}/[0.035(10^{-1})^3(3/6 \times 10^{-6})] \sim 10^{-5}$ m^{-1}, $D_L \sim 10^{-9}$ m^3/sPa, $D_{eff} \sim 10^{-7}$ m^2/s, and the left side of the inequality shown in Eq. (4) becomes approximately equal to 1.0. This result indicates that the lumped capacity model, from which the Krogh equation can be derived, is in the threshold of not being valid. This conclusion is corroborated by the deviation of the curve γ versus t from the straight dashed-line also shown in Fig. 1.

The generally short (about 10 seconds) time duration of the clinical single-breath test masks the deviation from the lumped capacity model. However, by allowing the numerical simulation to proceed further in time, the resulting D_L becomes time-dependent invalidating a fundamental hypothesis behind Eq. (3), i.e., constant D_L.
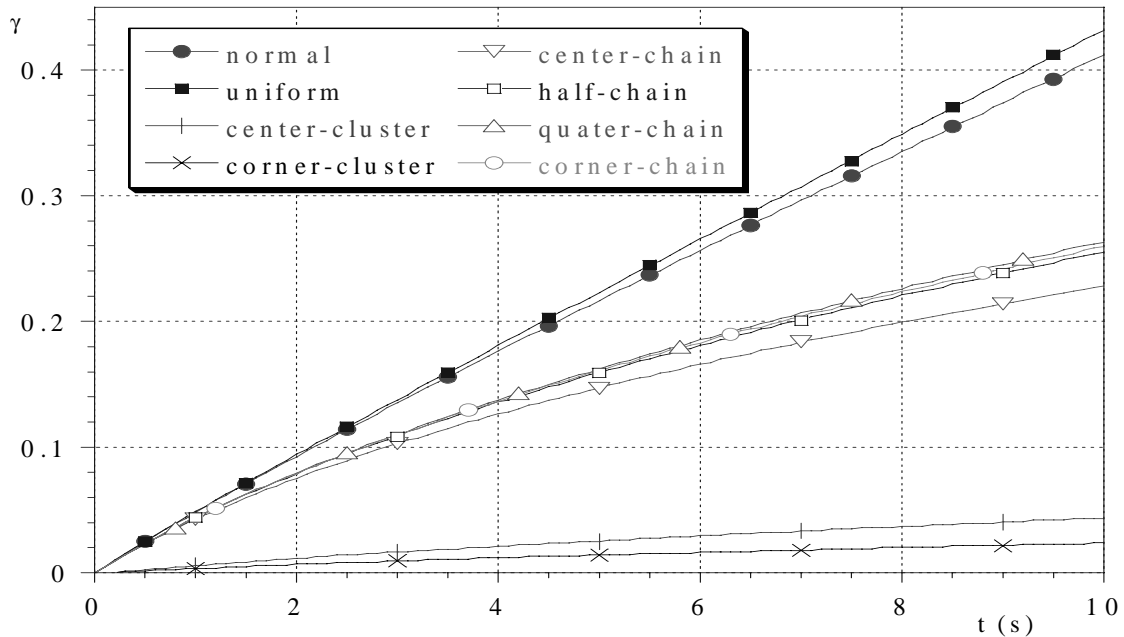

Figure 1 - Transient diffusion: comparison of uniform, normal, cluster, and chain red cell distributions, for $\rho = 3.4$ %. *Center, half, quarter, and corner*-chain distributions refer to the location of the first red cell of the chain.

6. OTHER RED CELL DISTRIBUTIONS

Observe that the RBC distribution within the alveolar domain does not alter the effective diffusivity of the domain (as long as the red cell density is the same), but it does affect the lung diffusing capacity. This is because the effective diffusivity, as defined, does not depend on where the red cells are within the domain, as they are simply internal boundaries for the diffusion process modeled by the macroscopic Eq. (1). Consequently, other red cell distributions can be simulated numerically once the effective diffusivity of the alveolar region is determined for a certain RBC density, as long as the red cell density is kept the same.

In the previous section, the effective diffusivity of the alveolar region for RBC density equal to 3.4 % was determined. Now, the transient CO diffusion process can be simulated considering other red cell distributions, for the same RBC density. The equivalent lung diffusing capacity for each RBC distribution can be calculated from Eq. (3), and compared to the base lung diffusing capacity, D_{L-n} = 17 ml$_{CO}$/(min mmHg), of normal (random) red cell distribution.

Initially, a uniform distribution is considered in which the RBC's are uniformly distributed in spaced within the domain. The resulting time-evolution of the partial-pressure for this case is shown in Fig. 1, next to the result for the normal distribution.

The transient numerical simulation yields, from Eq. (3), the value D_{L-u} = 17.9 ml$_{CO}$/(min mmHg) for the uniform distribution. In comparison with the lung diffusing capacity obtained from the normal RBC distribution, the D_L value from the uniform distribution is slightly higher. In fact, it would have been easy to anticipate the higher lung diffusing capacity of the uniform distribution because this distribution maximizes the volume of influence of each red cell within the domain, minimizing the competition for gas, which is characteristic of red cell clustering. The very small increase in D_L (approximately five percent) reveals that the normal (random) distribution of red cells yields a configuration similar to the configuration for optimum diffusion process obtained with uniformly distributed red cells.

To investigate the red cell clustering effect (reported by Koulich et al. (1999) for the case of steady diffusion), two other red cell distributions are investigated. They are the center-clustering and the corner-clustering distributions.

These distributions are obtained by clustering the red cells around the center of the domain or adjacent to one of the corners of the domain, respectively.

The time-evolution of the volume-averaged partial-pressure for these cases is shown in Fig. 1. Corresponding values of lung diffusing capacity, obtained using Eq. (3), are: D_{L-cec} = 1.79 ml$_{CO}$/(min mmHg) and D_{L-coc} = 0.99 ml$_{CO}$/(min mmHg), respectively for center and corner clustering. The two cluster results show radical reduction in D_L when compared to the uniform and normal red cell distributions. This is expected because the RBC's inside the cluster are shielded by the red cells on the periphery of the cluster, becoming less effective sinks of CO. This shielding effect was observed also during the simulations of the steady-state model by Koulich et al. (1999), and in the two-dimensional capillary simulations performed by Hsia et al. (1995).

Somewhat surprising is the strong effect of cluster-location on D_L. The corner-clustering configuration yields a low diffusion performance (lower than the center-clustering performance) because the RBC cluster is placed adjacent to the corner-boundary of the domain. That is, three out of the six cluster boundaries are left without access to CO. Therefore, one would expect that $D_{L-cec}/2 \sim D_{L-coc}$, a prediction confirmed approximately by the numerical results.

Obviously, one can expect the lung diffusing capacity to vary between D_{L-cec} and D_{L-coc} if the same cluster is placed anywhere else in the domain. Moreover, it is believed that the

corner cluster provides the worst possible red cell distribution configuration, yielding a lower bound value for the lung diffusing capacity. Assuming the D_L value for uniform red cell distribution as an upper bound value, the effect of red cell distribution on D_L then spreads itself within a range from 0.99 to 17.9 ml$_{CO}$/(min mmHg).

A different red cell distribution, called chain-type, is also investigated. The chain is formed by placing the red cells consecutively along a line in the domain, following a random path. Therefore, each red cell has at least one neighboring red cell. The starting point of the chain varies from the center to one of the corners of the domain, along one of the diagonals (see top right section of Fig. 2). A *half-chain* distribution refers to a chain having the first cell placed halfway between the center and the corner of the domain. A *quarter-chain* distribution refers to a chain having the first cell placed a quarter of half-diagonal length from the corner of the domain. Results of the volume-averaged partial-pressure evolution in time are summarized in Fig. 1.

Amazingly, the chain distributions yield similar lung diffusing capacity coefficients (see Table 1), distinct to what was observed when comparing the lung diffusing capacity of clustering distributions. It seems as if the starting location of the random chain is irrelevant to the lung diffusing capacity. It is possible, for this type of distribution, that the distance between red cells be a predominating factor.

Trying to quantify the location-versus-distance effect of red cell distribution, we devised two geometrical parameters to help characterize each distribution. The geometrical significance of these two parameters is better understood considering the simplified two-dimensional sketch shown in the lower right section of Fig. 2. One of these parameters is the distance between the geometrical center of the red cell distribution, defined by the coordinates (X_c, Y_c, Z_c), and the center of the domain at (X_0, Y_0, Z_0). The coordinates of the geometrical center of the red cell distribution are found from the equation

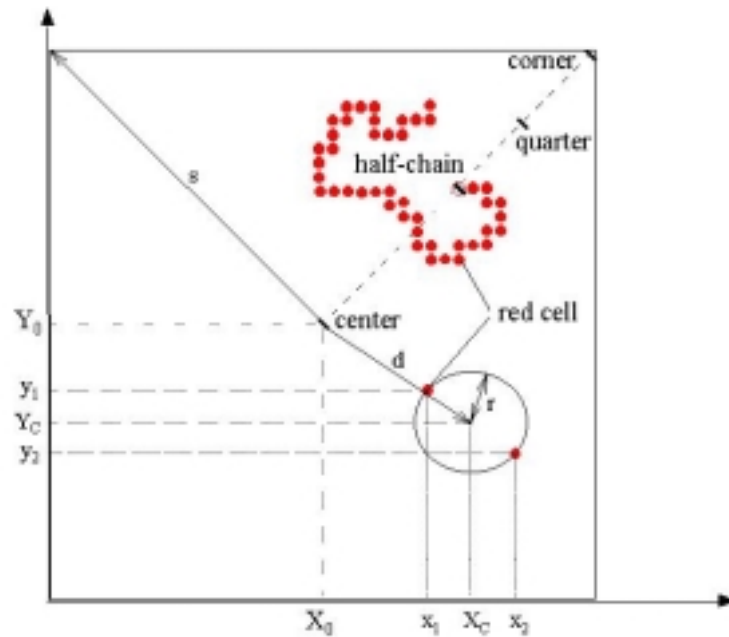$$(X_c, Y_c, Z_c) = \frac{1}{N} \sum_{i=1}^{N} (x_i, y_i, z_i)$$ (6)

Figure 2 - Two-dimensional schematic representation of *chain-type* red cell distributions: *center*, *half*, *quarter*, and *corner* refer to the location of the first red cell of the chain.

where (x_i, y_i, z_i) are the coordinates of each red cell, and N is the total number of red cells in the domain. Hence, the distance to the center of the domain is simply,

$$d = \left[(X_c - X_0)^2 + (Z_c - Z_0)^2 + (Z_c - Z_0)^2\right]^{1/2} \tag{7}$$

The other geometrical parameter characterizing the red cell distribution is the effective radius of the red cell distribution, r,

$$r = \left(r_x^2 + r_y^2 + r_z^2\right)^{1/2} \tag{8}$$

with,

$$\left(r_x, r_y, r_z\right) = \frac{1}{N} \sum_{i=1}^{N} \left[\left|(X_c - x_i)\right|, \left|(Y_c - y_i)\right|, \left|(Z_c - z_i)\right|\right] \tag{9}$$

One can see in Fig. 2 the representative distance d and radius distribution r for the two red cells shown in the figure. A large d-value indicates the cell distribution is far from the center, hence, close to the boundaries where the diffusion process is less effective. A small r-value indicates the red cells are close together, maybe forming a cluster, also leading to a less effective diffusion configuration. Hence, d and r are in principle two good candidates for quantifying the sensibility of the lung diffusing capacity to red cell distribution.

Values of d and r normalized in respect to the diagonal half-length of the domain, and values of D_L for each red cell distribution normalized by the normal D_L value are summarized in Table 1. Observe first that the uniform and center-clustering distributions are not perfectly centered in the domain. This is because the number of red cells necessary to reach 3.4 percent red cell density does not allow a perfectly symmetric distribution in relation to the center of the three-dimensional domain. The distortion caused by this effect, however, is minor.

Table 1. Normalized lung diffusing capacity, red cell distribution distance from the center of the domain d, and distribution radius r. D_{L-n} is the lung diffusing capacity of normal RBC distribution; s is the half-length of the diagonal of the alveolar domain (see Fig. 2).

Distribution:	D_L/D_{L-n}	d/s	r/s
Uniform	1.05	0.05	0.47
Normal	1.00	0.03	0.48
Cluster:			
Center	0.11	0.15	0.27
Corner	0.06	0.55	0.21
Chain:			
Center	0.56	0.31	0.42
Half	0.62	0.19	0.44
Quarter	0.64	0.20	0.44
Corner	0.63	0.24	0.42

Notice from Table 1 that the normal (random) and uniform distributions have very similar d and r, and that is why these two distributions yield very similar D_L. The d and r values for the two cluster distributions indicate that d, varying by 270 percent, is not very influential on the value of D_L, varying only 29 percent. This observation is confirmed also by the values of d for the chain distributions for which r is relatively constant, confirming our earlier expectation that the random chain path produces similar distributions in terms of r, independently from where the chain starts.

Based on these observations, the normalized lung diffusion values presented in Table 1 are plotted versus the normalized radius of distribution, shown in Fig. 3. The straight line is a polynomial curve-fit, namely

$$\frac{D_L}{D_{L-n}} = -1.6\frac{r}{s} + 19\left(\frac{r}{s}\right)^2 - 68\left(\frac{r}{s}\right)^3 + 93\left(\frac{r}{s}\right)^4 \tag{10}$$

Observe that 15 percent error bars are also depicted in Fig. 3, a deviation effect attributed to the parameter d not accounted for in Eq.(10).

7. SUMMARY AND CONCLUSIONS

By mimicking the single-breath experimental technique within a hypothetical cubic domain with 3.4 percent red cell distributed randomly (normal distribution), the iterative numerical simulation of the transient model leads to an effective diffusivity value equivalent to the measured lung diffusing capacity. With this effective diffusivity, a quantity independent of the red cell positioning within the domain, several red cell distributions are investigated.

The equivalent lung diffusing capacity of each red cell distribution is obtained, from the numerical results, using the Krogh equation. An analytical criterion for the validity of the single-breath lumped-capacity model is also presented.

Results for normal (random), uniform, center-clustering, corner-clustering, and four chain-like random distributions suggest a strong influence of red cell distribution over the lung diffusing capacity. The introduction of two descriptive geometrical parameters,
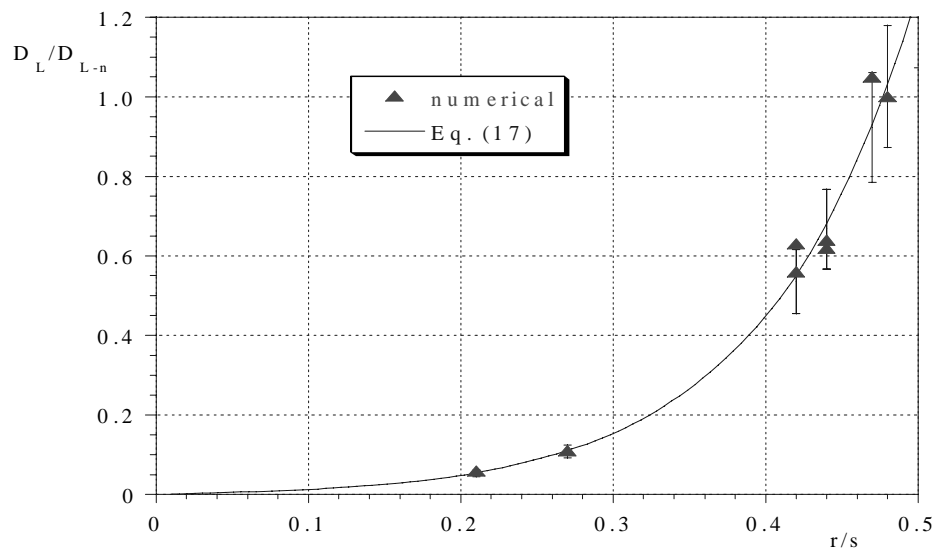

Figure 6 - Normalized lung diffusion coefficient versus normalized distribution radius, $\rho = 3.4\%$. Also shown are 15 percent-error vertical bars.

characterizing the red cell distributions, help identify the predominance of the distribution radius on the lung diffusing capacity. A polynomial correlation is proposed for estimating the distribution radius effect on the lung diffusing capacity.

It is concluded that the three-dimensional distribution of the red cells, characterized by the distribution radius, has a fundamental impact on the lung diffusing capacity. This conclusion indicates that the Roughton-Foster lung diffusing capacity model, used in physiology and morphometric analysis, must be re-interpreted in light of the red cell distribution effect within the alveolar region.

REFERENCES

Comroe, J. H., Forster, R. E., Dubuis, A. B., Briscoe, W. A. and Carlsen, E., 1962, The lung clinical physiology and pulmonary functions tests, Chicago, Year Book Medical Publisher, pp. 117–121.

Crapo, J. D., and R. O. Crapo, 1983, Comparison of total lung diffusion capacity and the membrane component of diffusion capacity as determined by physiologic and morphometric techniques, Respir. Physiol, vol. 51, pp. 183–194.

Crapo, J. D., R. O Crapo, R. L. Jensen, R. R. Mercer, and E. R. Weibel, 1988, Evaluation of lung diffusing capacity by physiological and morphometric techniques, J. Appl. Physiol, vol. 64, pp. 2083–2091.

Fedrespiel, W. J., 1989, Pulmonary diffusing capacity: implications of two-phase blood flow in capillaries, Respir. Physiol, vol. 77, pp. 119–134.

Hsia, C. C. W., C. J. C. Chuong, R. L. Johnson, Jr., 1995, Critique of conceptual basis of diffusing capacity estimates: a finite element analysis, J. Appl. Physiol, vol. 79, pp 1039–1047.

Johnson, R. L., Jr., W. S. Spicer, J. M. Bishop, and R. E. Forster, 1960, Pulmonary capillary blood volume, flow, and diffusing capacity during exercise, J. Appl. Physiol., vol. 15, pp. 893–902.

Koulich, V.V., 1999, Heat and Mass Diffusion in Microscale: Fractals, Brownian Motion, and Fractional Calculus, Ph. D. Dissertation, Mechanical Engineering Department, Southern Methodist University.

Koulich, V.V., J.L. Lage, C.C.W. Hsia, and R.L. Johnson, Jr.., 1999, A Porous Medium Model of Alveolar Gas Diffusion, J. Porous Medium, vol. 2, pp. 263-275.

Newth, C. J. L., D. J. Cotton, and J. A. Nadel, 1977, Pulmonary diffusing capacity measured at multiple intervals during a single exhalation in man, J. Appl. Physiol., vol. 43, pp. 617–625.

Roughton, F. J. W., and R. E. Foster, 1957, Relative importance of diffusion and chemical reaction rates in determining the rate of exchange of gases in the human lung, with special reference to true diffusing capacity of the pulmonary membrane and volume of blood in lung capillaries, J. Appl. Physiol., vol. 11, pp. 290–302.

Weibel, E. R., 1970, Morphometric estimation of pulmonary diffusion capacity. I. Model and method, Respir. Physiol., vol. 11, pp.54–75.

Weibel, E. R., W. J. Federspiel, F. Fryder-Doffey, C. C. W. Hsia, M. Konig, V. Stalder-Navarro, and R. Vock, 1993, Morphometric model or pulmonary diffusing capacity. I. Membrane diffusing capacity, Respir. Physiol., vol. 93, pp. 125–149.

American Thoracic Society, 1987, Single breath carbon monoxide diffusing capacity (transfer factor): recommendations for a standard technique, Am. Rev. Respir. Dis., vol. 136, pp. 1299–1307.